Shape-Selective Separation of Molecular Isomers with Tunable Hydrogen-Bonded Host Frameworks

Adam M. Pivovar, K. Travis Holman, and Michael D. Ward*

Department of Chemical Engineering and Materials Science, University of Minnesota, Amundson Hall, 421 Washington Avenue SE, Minneapolis, Minnesota 55455

Received May 3, 2001. Revised Manuscript Received June 18, 2001

The propensity of hydrogen-bonded guanidinium (**G**) organodisulfonates (**S**) to form crystalline inclusion compounds has been investigated in the context of separating isomeric mixtures of xylenes and dimethylnaphthalenes via selective inclusion. Pairwise competition experiments, in which inclusion compounds are grown from solutions containing an isomeric mixture of guests, map the inclusion selectivity of a particular host as a function of guest content in solution. Whereas the $\mathbf{G}_2$[4,4′-biphenyldisulfonate] host is minimally selective with respect to inclusion of *o*-, *m*-, or *p*-xylene, the homologous $\mathbf{G}_2$[2,6-naphthalenedisulfonate] is highly selective toward the inclusion of *p*-xylene, by a factor of 36 and 160 versus *o*-xylene and *m*-xylene, respectively. Similarly, the hosts of the homologous series $\mathbf{G}_2$[2,6-naphthalenedisulfonate], $\mathbf{G}_2$[4,4′-biphenyldisulfonate], $\mathbf{G}_2$[2,6-anthracenedisulfonate], and $\mathbf{G}_2$[4,4′-azobenzenedisulfonate] display different selectivity for the 10 isomers of dimethylnaphthalene. The details of the selectivity behavior are highly dependent on the molecular structure of the **GS** host and the solid-state structures of the corresponding inclusion compounds. Single crystal structure determinations reveal that isomer selectivity is most pronounced when the structures of corresponding inclusion compounds are significantly different, i.e., when the isomeric guests template different architectural isomers of the host. Furthermore, selectivity appears to be a consequence of size and shape compatibility between the host and guest. The observation of selective inclusion demonstrates the feasibility of a crystallization-based separation process based on these host compounds.

Introduction

The separation of multicomponent mixtures into their individual components typically involves exploiting differences in a specific physical property. Distillation, crystallization, and liquid−liquid extractions are commonly employed unit operations that isolate constituents of a mixture based on differences in volatility or solubility. If the components of a mixture have extremely similar properties, as is generally the case for molecular isomers, traditional separation methods can be unfeasible to the extent that less conventional approaches, such as selective sorption or inclusion within a host material, may be required. Whereas traditional porous materials, such as inorganic zeolites, have been studied extensively and have achieved considerable commercial success in this respect,[1] modern "designer" inclusion materials, such as molecule-based organic[2,3] and metal-organic[4] hosts, also hold considerable promise for selective inclusion. Unlike covalent host frameworks, which rely on selective sorption and diffusion through preexisting pores, the "pores" in noncovalent frameworks are typically created during assembly of the crystalline inclusion compound and are generally only sustainable when occupied by guest molecules.[5] Nevertheless, if the host is selective, the preferentially included guest can be separated from a solution mixture by filtration of the crystallized inclusion compound. The guest can then be retrieved, for example by dissolution and extraction, under mild conditions and the host material can be recycled (Scheme 1).

Organic or molecular hosts are particularly appealing candidates for selective inclusion because their general solubility allows for both effective retrieval of included

* To whom correspondence should be addressed.

(1) (a) Guo, Q.-Q.; Chen, H.; Long, Y.-C. *Micropor. Mesopor. Mater.* **2000**, *39*, 149. (b) Padin, J.; Yang, R. T. *Chem. Eng. Sci.* **2000**, *55*, 2607. (c) Lee, H.-R.; Tan, C.-S. *Ind. Eng. Chem. Res.* **2000**, *39*, 1035.

(2) (a) Atwood, J. L.; Davies, J. E. D.; MacNicol, D. D., Eds. *Inclusion Compounds, Vol. 2* (*Structural Aspects of Inclusion Compounds Formed by Organic Host Lattices*); Academic Press: London, 1984. (b) Weber, E.; Josel, H.-P. *J. Inclusion Phenom.* **1983**, *1*, 79. (c) Weber, E. *Top. Cur. Chem.* **1987**, *140*, 1−20. (d) Bishop, R. *Chem. Soc. Rev.* **1996**, *25*, 311. (e) Aoyama, Y. *Top. Curr. Chem.* **1998**, *198*, 131−161. (f) Herbstein, F. H. *Acta Chim. Hung.* **1993**, *130*, 377.

(3) (a) Weber, E. *Top. Curr. Chem.* **1988**, *149*, 45−135 (b) Weber, E. In *Comprehensive Supramolecular Chemistry;* Atwood, J. L., Davies, J. E. D., MacNicol, D. D., Vögtle, F., Suslick, K. S., Eds.; Elsevier: Oxford, 1996; Vol. 6, pp 535−592. (c) Ermer, O.; Lindenberg, L. *Helv. Chim. Acta* **1991**, *74*, 825−877. (d) Jetti, R. K. R.; Kuduva, S. S.; Reddy, D. S.; Xue, F.; Mak, T. C. W.; Nangia, A.; Desiraju, G. R. *Tetrahedron Lett.* **1998**, *39*, 913−916.

(4) (a) Zaworotko, M. J. *Chem. Commun.* **2001**, 1−9. (b) Robson, R. *Dalton* **2000**, 3735−3744. (c) Hagrman, P. J.; Hagrman, D.; Zubieta, J. *Angew. Chem., Int. Ed.* **1999**, *38*, 2639−2684. (d) O'Keeffe, M.; Eddaoudi, M.; Li, H.; Reineke, T.; Yaghi, O. M. *J. Solid State Chem.* **2000**, *152*, 3−20. (e) Batten, S. R.; Robson, R. *Angew. Chem., Int. Ed.* **1998**, *37*, 1461−1494.

(5) Some examples of molecule-based materials which maintain structural integrity upon guest removal have been recently reported: (a) Eddaoudi, M.; Moler, D. B.; Li, H.; Chen, B.; Reineke, T. M.; O'Keeffe, M.; Yaghi, O. M. *Acc. Chem. Res.* **2001**, *34*, 319−330. (b) Brunet, P.; Simard, M.; Wuest, J. D. *J. Am. Chem. Soc.* **1997**, *119*, 2737−2738. (c) Chui, S. S.-Y.; Lo, S. M.-F.; Charmant, J. P. H.; Orpen, A. G.; Williams, I. D.; *Science* **1999**, *283*, 1148−1150. (d) Noro, S.; Kitagawa, S.; Kondo, M.; Seki, K. *Angew. Chem., Int. Ed.* **2000**, *39*, 2082−2084.

10.1021/cm0104452 CCC: $20.00
Published on Web 08/21/2001

Scheme 1

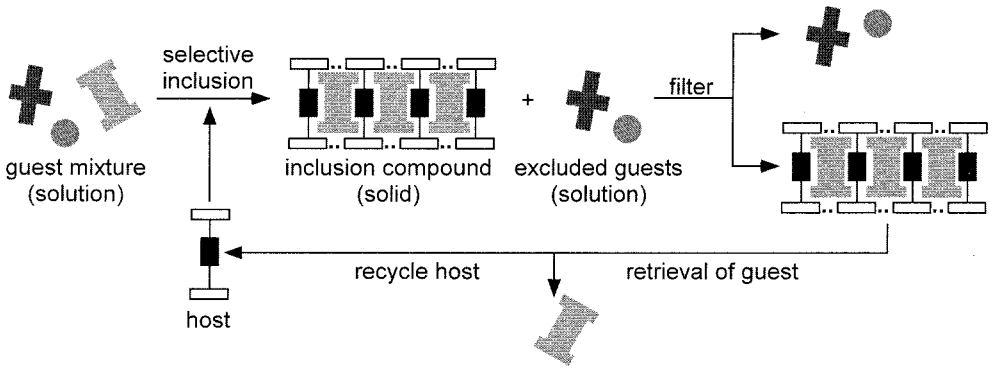

guests and recycling of the host material. Serious limitations still exist, however, with respect to the design of an appropriate organic host for a particular separations application. For example, many traditional organic hosts, such as (thio)urea,[6] tri-*o*-thymotide,[7] Dainin's compound,[8] perhydrotriphenylene,[9] and cyclotriveratrylene,[10] cannot be chemically modified or tailored without the concomitant loss of the inclusion capabilities of the host. Although some molecular hosts, such as Werner complexes[11] and many diol hosts,[12,13] are amenable to chemical modification, such modifications rarely lead to *predictable* changes in the size or shape of the inclusion cavities. Therefore, even though numerous inclusion hosts are available[2] and strategies for the de novo molecular-level design of hosts have been proposed,[3] a particular separation typically requires the design and testing of a variety of hosts,[13] frequently with rather disparate compositions and architectures. In contrast, libraries of homologous inclusion hosts, in which the composition of the host is systematically adjusted but key architectural features are retained, may provide a route to effective and facile optimization of a particular separation.

We have recently reported a family of homologous inclusion hosts that fulfill the above criteria.[14] Guanidinium (**G**) salts of organosulfonate anions (**S**) consistently form lamellar motifs by virtue of hydrogen bonding between the N−H moieties of the **G** cations and the sulfonate moieties of the **S** anions.[14,15] The H-bonded **GS** lamellae adopt either a "quasi-hexagonal" arrangement (Scheme 2) that embodies the complementary symmetries of the **G** ions (D_{3h}) and the sulfonate moieties (C_{3v}), or a closely related, albeit less common, "shifted-ribbon" motif (not shown). In either arrangement, the **GS** lamellae can be pillared in the third dimension by the readily modified organic residues of organo*di*sulfonate anions, thereby creating inclusion cavities between the sheets that are occupied by guest molecules during assembly of the **GS** host lattice.

The lamellar character of the **GS** host framework persists for a diverse collection of pillars and guests, a feature that can be partially attributed to an inherent conformational flexibility of the **GS** sheet that allows the host to adapt to the size and shape of different guest molecules. The primary deformation mechanism of the flexible **GS** sheet is a pleatlike puckering, whereby the sheets fold about an axis of hydrogen bonds connecting adjacent rigid one-dimensional **GS** "ribbons." Whereas the lattice dimension along the rigid **GS** ribbons (a_1) is essentially constant (7.5 ± 0.2 Å), the lattice parameter orthogonal to the ribbon direction (b_1) is variable and depends on the degree of puckering, which is defined by the "inter-ribbon puckering angle", θ_{IR}.

One of the more interesting features of the **GS** hosts is their architectural isomerism, the two most

(6) (a) Harris, K. D. M. *Chem. Soc. Rev.* **1997**, *26*, 279−290. (b) Hollingsworth, M. D.; Harris, K. D. M. In *Comprehensive Supramolecular Chemistry Chemistry*; Atwood, J. L., Davies, J. E. D., MacNicol, D. D., Vögtle, F., Suslick, K. S., Eds.; Elsevier: Oxford, 1996; Vol. 6, pp 177−237.

(7) (a) Gerdil, R. In *Comprehensive Supramolecular Chemistry Chemistry*; Atwood, J. L., Davies, J. E. D., MacNicol, D. D., Vögtle, F., Suslick, K. S., Eds.; Elsevier: Oxford, 1996; Vol. 6, pp 239−280. (b) Gerdil, R. *Top. Curr. Chem.* **1987**, *140*, 71−105.

(8) MacNicol, D. D. In *Inclusion Compounds*; Atwood, J. L., Davies, J. E. D., MacNicol, D. D., Eds.; Academic Press: London, 1984; Vol. 2, pp 1−45.

(9) (a) Hulliger, J.; Roth, S. W.; Quintel, A.; Bebie, H. *J. Solid State Chem.* **2000**, *152*, 49−56. (b) Farina, M.; Di S. G.; Sozzani, P. In In *Comprehensive Supramolecular Chemistry*; Atwood, J. L., Davies, J. E. D., MacNicol, D. D., Vögtle, F., Suslick, K. S., Eds. Elsevier: Oxford, 1996; Vol. 6, pp 371−398. (c) Farina, M. In *Inclusion Compounds*; Atwood, J. L., Davies, J. E. D., MacNicol, D. D., Eds.; Academic Press: London, 1984; Vol. 2, pp 69−95.

(10) (a) Collet, A. In *Comprehensive Supramolecular Chemistry Chemistry*; Atwood, J. L., Davies, J. E. D., MacNicol, D. D., Vögtle, F., Suslick, K. S., Eds. Elsevier: Oxford, 1996; Vol. 6, pp 281−303. (b) Collet, A.; Dutasta, J.-P.; Lozach, B.; Canceill, J. *Top. Curr. Chem.* **1993**, *165*, 103−29. (c) Collet, A. *Tetrahedron* **1987**, *43*, 5725−5759. (d) Collet, A. In *Inclusion Compounds*; Atwood, J. L., Davies, J. E. D., MacNicol, D. D., Eds.; Academic Press: London, 1984; Vol. 2, pp 97−121.

(11) (a) Schaeffer, W. D.; Dorsey, W. S.; Skinner, D. A.; Christian, C. G. *J. Am. Chem. Soc.* **1957**, *79*, 5870−5876. (b) Williams, F. V. *J. Am. Chem. Soc.* **1957**, *79*, 5876−5877. (c) Lipkowski, J. In *Comprehensive Supramolecular Chemistry Chemistry*; Atwood, J. L., Davies, J. E. D., MacNicol, D. D., Vögtle, F., Suslick, K. S., Eds.; Elsevier: Oxford, 1996; Vol. 6, pp 691−714.

(12) (a) Toda, F. In *Comprehensive Supramolecular Chemistry Chemistry*; Atwood, J. L., Davies, J. E. D., MacNicol, D. D., Vögtle, F., Suslick, K. S., Eds.; Elsevier: Oxford, 1996; Vol. 6, pp 465−516.

(13) (a) Caira, M. R.; Horne, A.; Nassimbeni, L. R.; Toda, F. *J. Mater. Chem.* **1997**, *7*, 2145. (b) Caira, M. R.; Horne, A.; Nassimbeni, L. R.; Toda, F. *J. Mater. Chem.* **1998**, *8*, 1481. (c) Caira, M. R.; Nassimbeni, L. R.; Vujovic, D.; Toda, F. *J. Phys. Org. Chem.* **2000**, *13*, 75. (d) Caira, M. R.; Nassimbeni, L. R.; Toda, F.; Vujovic, D. *J. Am. Chem. Soc.* **2000**, *122*, 9367. (e) Deng, J.; Chi, Y.; Fu, F.; Cui, X.; Yu, K.; Zhu, J.; Jiang, Y. *Tetrahedron: Asymmetry* **2000,** *11*, 1729. (f) Deketov, K.; Weber, E.; Seidel, J.; Köhnke, K.; Makhkamov, K.; Ibragimov, B. *Chem. Commun.* **1999**, 91.

(14) (a) Swift, J. A.; Pivovar, A. M.; Reynolds, A. M.; Ward, M. D. *J. Am. Chem. Soc.* **1998**, *120*, 5887. (b) Holman, K. T.; Pivovar, A. M.; Swift, J. A.; Ward, M. D. *Acc. Chem. Res.* **2001**, 34, 107−118. (c) Swift, J. A.; Reynolds, A. M.; Ward, M. D. *Chem. Mater.* **1998**, *10*, 4159. (d) Russell, V. A.; Evans, C. C.; Li, W.; Ward, M. D. *Science* **1997**, *276*, 575. (e) Holman, K. T.; Ward, M. D. *Angew. Chem., Int. Ed.* **2000**, *39*, 1653. (f) Evans, C. C.; Sukarto, L.; Ward, M. D. *J. Am. Chem. Soc.* **1999**, *121*, 320. (g) Swift, J. A.; Ward, M. D. *Chem. Mater.* **2000**, *12*, 150.

(15) (a) Russell, V. A.; Etter, M. C.; Ward, M. D. *J. Am. Chem. Soc.* **1994**, *116*, 1941−1952. (b) Russell, V. A.; Etter, M. C.; Ward, M. D. *Chem. Mater.* **1994**, *6*, 1206−1217. (c) Russell, V. A.; Ward, M. D. *J. Mater. Chem.* **1997**, *7*, 1123−1133.

Scheme 2

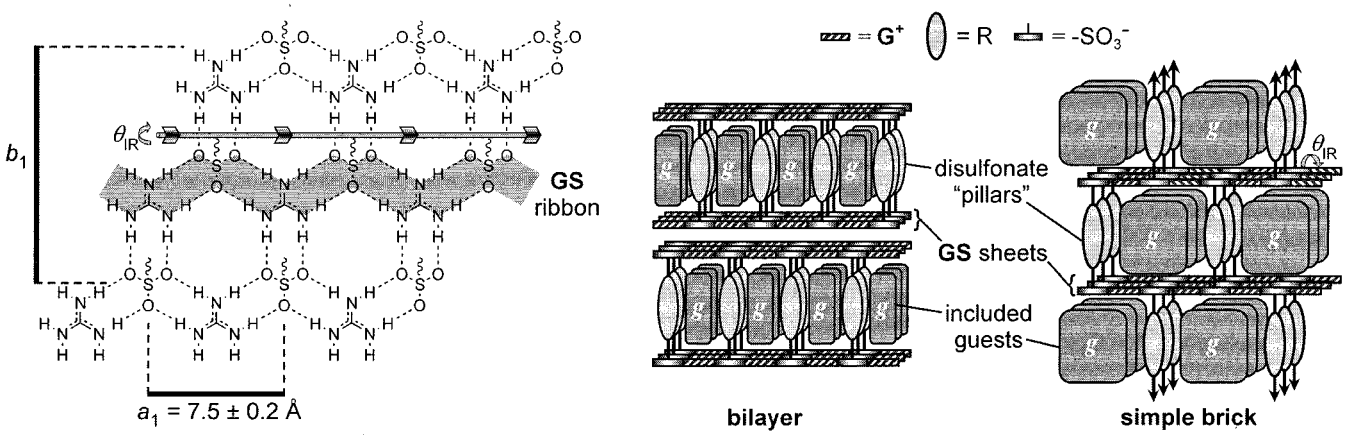

common isomers being the discrete "bilayer" and continuous "simple brick" forms (Scheme 2).[14a,b,16] For a given organodisulfonate pillar, the simple brick host framework has a lower density and is capable of including larger guests or greater numbers of guests than the bilayer form. The ease with which the organodisulfonate pillars can be structurally modified, coupled with this architectural isomerism, affords a diverse library of hosts with variable inclusion cavity sizes and shapes.

The use of **GS** hosts for the selective inclusion of simple molecular isomers that are difficult to separate by traditional methods, namely the three xylenes and the 10 dimethylnaphthalenes, is described herein. This approach relies on a small library of host compounds that includes $\mathbf{G_2NDS}$, $\mathbf{G_2BPDS}$, $\mathbf{G_2ADS}$, and $\mathbf{G_2ABDS}$ (**NDS** = 2,6-naphthalenedisulfonate; **BPDS** = 4,4′-biphenyldisulfonate; **ADS** = 2,6-anthracenedisulfonate; **ABDS** = 4,4′-azobenzenedisulfonate). Although it is a trivial exercise to demonstrate that these **GS** hosts can be used to separate molecules of substantially different size, the separation of molecules with essentially identical volumes and physical properties is considerably more challenging as it must rely on subtle differences in shape recognition by the inclusion cavities of the host. The ability to tailor the **GS** family of hosts through choice of the organodisulfonate pillar provides a key advantage in this respect. Furthermore, the molecular isomers considered here are lacking in "sticky" (e.g., H-bonding) chemical functionality that would allow use of *coordinato*-clathrate concepts,[3a,b] wherein a host is designed to interact with or complex a guest via specific and directional noncovalent interactions. Overall, the results demonstrate that selectivity between a given pair of isomers is most pronounced if the different isomers template different architectures of the host, illustrating a key advantage of separations based on hosts that themselves can form architectural isomers of identical composition and containing a common structural element, in this case the **GS** sheet. In the case of the **GS** hosts, this is achieved by choosing a host that straddles the steric boundary between two host architectures for a particular set of guest isomers.

Results and Discussion

Selectivity and Separation Protocol. Separation protocols based upon selective inclusion require that the host exhibit some preference for inclusion of one particular guest over another. Crystals of the corresponding inclusion compound, grown from a solution containing a mixture of guests, would thus be enriched in one of the guests, whereas the filtrate solution would become enriched in the other guest. Pairwise competition experiments, wherein inclusion compounds are grown from a series of solutions of known guest composition, can be used to determine the dependence of inclusion selectivity on the solution content of the two guests (A and B). The selective preference of a host (**H**) for one compound (A) from the mixture can be described by a *selectivity coefficient* ($K_{A:B}$), defined according to eq 1, where X_A and X_B represent the mole fractions of the two competing guests in the original solution and Y_A and Y_B represent the corresponding mole fractions of the same guests in the resulting inclusion compound. If the selectivity coefficient is constant over the entire range of X_A, the selectivity profile will be symmetrical about a line drawn from the lower right to the upper left corners, as depicted for curves (a−d) of increasing $K_{A:B}$ in Figure 1. It is reasonable to expect that this condition will exist if the corresponding inclusion compounds, $\mathbf{H}\cdot(A)_n$ and $\mathbf{H}\cdot(B)_m$, are isostructural throughout the entire range of X_A, that is, if $\mathbf{H}\cdot(A)_{n-x}(B)_x$ has essentially the same structure as $\mathbf{H}\cdot(B)_{m-y}(A)_y$ for all values of x and y ($x < n$; $y < m$). Indeed, symmetrical Y_A vs X_A curves are a common feature of host materials with preexisting pores wherein the host structure is unchanged by guest inclusion.[1a] The $K_{A:B}$ of molecular hosts, however, often depends significantly on the relative concentrations of guests in the original solution mixture, affording less symmetrical curves such as that depicted in curve (e) of Figure 1.[13] Asymmetric curves can reflect the formation of structurally dissimilar inclusion compounds $\mathbf{H}\cdot(A)_n$ and $\mathbf{H}'\cdot(B)_m$, where **H** and **H**′ represent different host architectures. For example, curve (e) illustrates that guest B is included preferentially at low X_A, forming crystals of $\mathbf{H}'\cdot(B)_{m-y}(A)_y$ that are isostructural with $\mathbf{H}\cdot(B)_m$. At higher values of X_A, guest A is included preferentially as the system produces crystals of

(16) We have also recently discovered a considerable number of other architectural isomers—referred to as "crisscross bilayer", "double-brick", "zigzag brick", and "V-brick"—which differ with respect to either the topological projection (i.e., the up−down arrangement) of the organodisulfonate pillars from the **GS** sheets or the connectivity between the sheets: Holman, K. T.; Martin, S. M.; Parker, D. P.; Ward, M. D. *J. Am. Chem. Soc.* **2001,** *123,* 4421−4431.

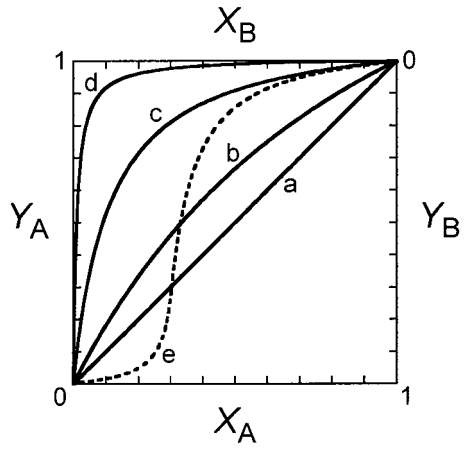

Figure 1. Pairwise competition experiments can be used to map the inclusion selectivity of one guest (A) relative to another (B). The mole fractions of guests in the inclusion compound (Y_A or Y_B) are plotted as a function of the mole fraction of guests in the original solution mixture (X_A or X_B). The selectivity coefficient, $K_{A:B}$ (or $K_{B:A}$) can be extracted from any point on the curve. Larger selectivity coefficients correspond to a greater enrichment of guest A in the inclusion compound. (a) $K_{A:B} = 1$ (no selectivity), (b) $K_{A:B} = (K_{B:A})^{-1} = 2$, (c) $K_{A:B} = (K_{B:A})^{-1} = 10$, (d) $K_{A:B} = (K_{B:A})^{-1} = 100$. (e) $K_{A:B}$ is concentration dependent. Under conditions of low X_A ($0 < X_A < 0.3$) guest B is preferentially included ($K_{A:B} < 1$). At larger X_A ($0.3 > X_A > 1$) the selectivity is inverted ($K_{A:B} > 1$) and guest A is included preferentially.

H·$(A)_{n-x}(B)_x$ which have a structure similar to **H**·$(A)_n$, but different from **H′**·$(B)_m$.

$$K_{A:B} = (K_{B:A})^{-1} = Y_A/Y_B \cdot X_B/X_A \quad (X_A + X_B = 1) \quad (1)$$

The inclusion selectivity of molecular isomers by **GS** hosts was examined by pairwise competition experiments, wherein crystals of inclusion compounds were retrieved from methanolic solutions containing a particular **GS** host and a combined excess of guest isomers. The mole fractions of the two guests were varied, in increments of one tenth, from zero to one. The isomer compositions in the crystallized inclusion compounds were determined by gas chromatography and plotted in a manner identical to Figure 1, with X_{guest} and Y_{guest} representing the mole fractions of one of the guests in the original solution and the inclusion compound, respectively.

Selective Inclusion of Xylenes. Previous single-crystal X-ray diffraction studies by our laboratory demonstrated that **G**$_2$**BPDS** will form 1:1 inclusion compounds with all three isomers of xylene.[14c] The compounds **G**$_2$**BPDS**·(*o*-xylene), **G**$_2$**BPDS**·(*m*-xylene), and **G**$_2$**BPDS**·(*p*-xylene) are essentially isostructural. Each structure adopts the bilayer architecture, exhibits the "shifted-ribbon"[14c] **GS** sheet motif, and has xylene guests confined to one-dimensional channels flanked by the **BPDS** pillars (Figure 2). There are, however, subtle differences between the structures. First, the bilayer heights, as defined by the average positions of the guanidinium ions and the sulfonate moieties, are slightly different (11.0, 11.3, and 11.2 Å, respectively), reflecting differences in the tilt angles of the **BPDS** pillars. More importantly, however, are the subtle differences that arise as a consequence of the pillar−guest packing within the channels. For example, the guest molecules pack in a centrosymmetric arrangement within the channels of **G**$_2$**BPDS**·(*o*-xylene) and **G**$_2$**BPDS**·(*p*-xylene), but pack within the channels of **G**$_2$**BPDS**·(*m*-xylene) to form polar layers. Also, the aromatic rings of the **BPDS** pillars in **G**$_2$**BPDS**·(*p*-xylene) are coplanar, whereas they are significantly twisted in both **G**$_2$**BPDS**·(*o*-xylene) ($\tau = 20.0°$) and **G**$_2$**BPDS**·(*m*-xylene) ($\tau = 26°$ and 29°).

Pairwise competition experiments were employed to determine the selectivity of the **G**$_2$**BPDS** host toward the different xylene isomers. The selectivity profiles for each competition experiment are depicted in Figure 3a, plotting the mole fraction of a particular guest included in the host (Y) for a given mole fraction of the same guest in the initial crystallization medium (X). The data reveal that the **G**$_2$**BPDS** host exhibits only modest selectivity, in the order of *p*-xylene > *o*-xylene > *m*-xylene. In each case, the selectivity profiles are nearly symmetrical, with selectivity coefficients $K_{p-xyl:o-xyl} = 2.2$, $K_{p-xyl:m-xyl} = 1.7$, and $K_{o-xyl:m-xyl} = 1.5$.[17] Accordingly, crystallization of **G**$_2$**BPDS** from methanolic solutions containing an equimolar ratio of the three isomers affords a slight enrichment of the *para* and *ortho* isomer in the crystallized inclusion compound and a corresponding slight enrichment of the *meta* isomer in the filtrate. This behavior is depicted qualitatively in Figure 3a by the offset of the triangle, toward *o*- and *p*-xylene, from the center of diagram. That **G**$_2$**BPDS** does not effectively discriminate between the xylene isomers is perhaps not surprising given that the three **G**$_2$**BPDS**·(xylene) inclusion compounds are essentially isostructural. Previous efforts in our laboratory established the dependence of the host architecture on the relative size of the pillar and guest, with shorter pillars favoring the brick host architecture for a given guest. This prompted us to examine the selective inclusion of xylene isomers within **G**$_2$**NDS**, a **GS** host constructed with a pillar that is 2.1 Å shorter than **BPDS**.[14]

G$_2$**NDS** forms a 1:1 inclusion compound with *p*-xylene, the crystal structure revealing a bilayer architecture that is similar to that observed for the analogous **G**$_2$**BPDS** inclusion compound (Figure 4; Table 1).[16] The bilayer height (9.6 Å), however, is significantly smaller than that observed in **G**$_2$**BPDS**·(*p*-xylene), reflecting the shorter length of the **NDS** pillar. Furthermore, the S−C bond vectors of the **NDS** are essentially normal to the plane of the hydrogen-bonded **GS** sheet, indicating that the volumes of the host cavities are nearly maximal for the bilayer architecture of **G**$_2$**NDS**.

We have previously demonstrated that guests too "large" to fit within the bilayer architecture of a given **GS** host will template the brick architecture. It is important to note, however, that prediction of the host architecture for guest molecules with volumes that are near this critical bilayer-to-brick volume can be difficult. Near this threshold subtle packing factors may govern the host architecture to the extent that different archi-

(17) A selectivity coefficient, K, can be assigned for each data point on the respective competition plots. The values reported are averages of the selectivity coefficients obtained from the points in the regions of X specified. It should be noted that, owing to the limited amount of data, extremely small variations in the experimental values of Y lead to large differences in the calculated selectivity coefficients. Consequently, the errors associated with K can be as high as ±60%.

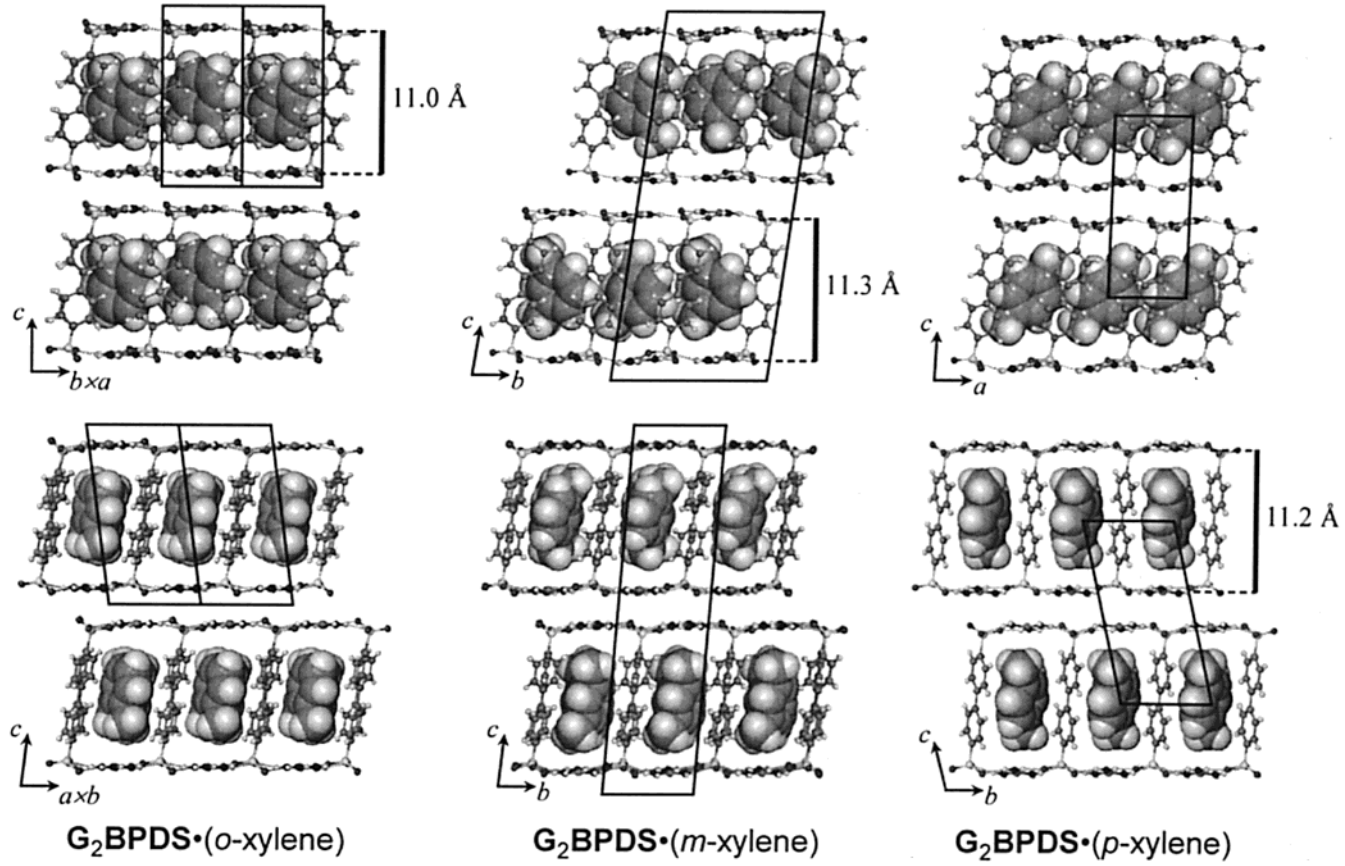

Figure 2. Bilayer organization observed in the single-crystal structures of **G$_2$BPDS**·(*o*-xylene), **G$_2$BPDS**·(*m*-xylene), and **G$_2$BPDS**·(*p*-xylene), as viewed roughly normal to (upper) and down (lower) the guest-occupied channels. The **GS** host frameworks and included guests are depicted by ball-and-stick and space-fill representations, respectively.

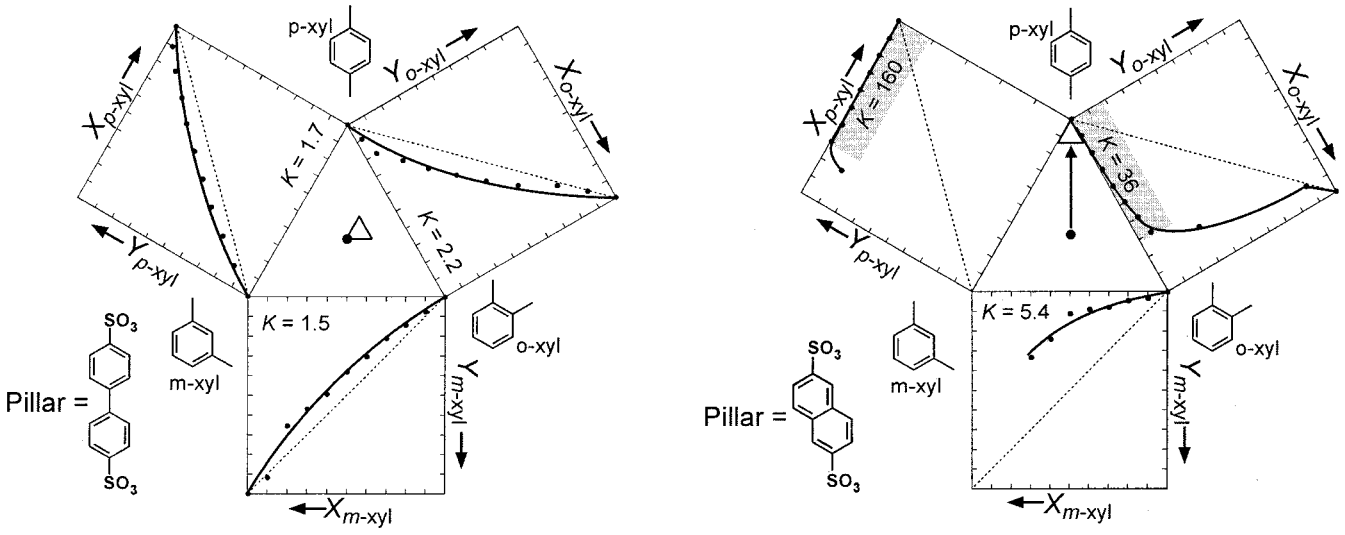

Figure 3. (a) Selectivity profiles for the inclusion of xylene isomers by **G$_2$BPDS**. The results of pairwise competition experiments are depicted as points on the plots at the periphery of the central triangle. The offset of the triangle from the filled circle in the center depicts the selectivity observed when competition experiments are performed with an equimolar ratio of all three isomers. The smooth curves represent average selectivity coefficients derived from the point data ($K_{p-\text{xyl}:o-\text{xyl}} = 2.2$, $K_{p-\text{xyl}:m-\text{xyl}} = 1.7$, and $K_{o-\text{xyl}:m-\text{xyl}} = 1.5$). (b) Selectivity profiles for the inclusion of xylene isomers by **G$_2$NDS**. The smooth curve for the *m*-xylene/*o*-xylene competition represents an average selectivity coefficient of $K_{o-\text{xyl}:m-\text{xyl}} = 5.4$. The selectivity profiles for *p*-xylene/*m*-xylene and *p*-xylene/*o*-xylene competitions are highly concentration dependent, and the curves represent an arbitrary best fit of the data in these instances.

tectures may be possible for isomeric guests of identical volume. For example, we have shown that the achievement of herringbone pillar−guest packing, typical of simple arenes,[18] governs the structure of some **GS** inclusion compounds with isomorphous arene guests and pillars.[14e] Interestingly, in contrast to the *p*-xylene,

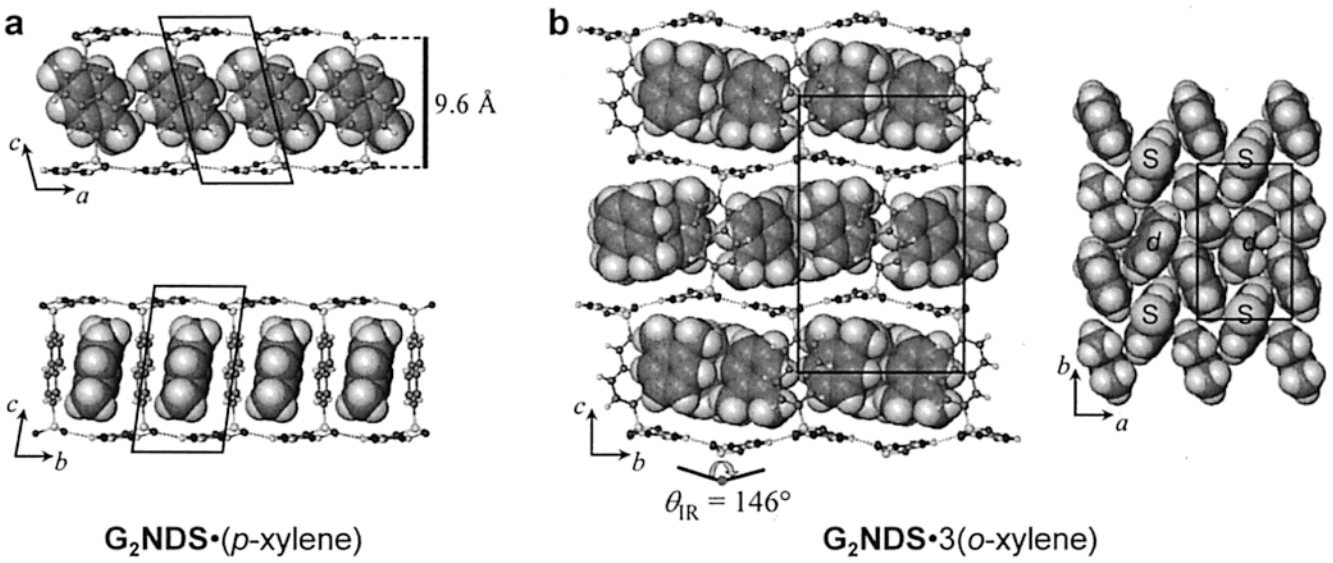

Figure 4. (a) The crystal structure of the bilayer inclusion compound **G**$_2$**NDS**·(*p*-xylene) as viewed down (lower) and roughly orthogonal to (upper) the guest occupied channels. (b) The crystal structure of the simple brick inclusion compound **G**$_2$**NDS**·3(*o*-xylene). Puckering of the **GS** sheets is denoted by the inter-ribbon puckering angle, θ_{IR}. The herringbone packing of **NDS** pillars (S) and *o*-xylene guests between the **GS** lamellae is depicted to the right. One-third of the *o*-xylene guests in the structure—those labeled as *d*—are disordered equally over the two orientations shown. Guanidinium ions and sulfonate oxygen atoms have been removed for clarity.

the inclusion compound of *o*-xylene with **G**$_2$**NDS** adopts the simple brick architecture, with 3 equiv of *o*-xylene in the larger inclusion cavities (Figure 4).[16] As in most simple brick structures, the **GS** sheets are puckered, with θ_{IR}, the dihedral angle between adjacent **GS** ribbons, measuring 146°. Notably, the observed unit cell volume (V_{cell}) of 1892 Å^3 is roughly 100 Å^3 less than the maximum value that can be obtained by this host.[19]

Several attempts to crystallize a *m*-xylene inclusion compound of **G**$_2$**NDS** proved unsuccessful. NMR and gas chromatographic analyses revealed that the solid product harvested from methanol solutions of **G**$_2$**NDS** and *m*-xylene (evaporated to near dryness) did not contain *m*-xylene.

The selectivity profiles for inclusion of xylene isomers by **G**$_2$**NDS** are depicted in Figure 3b. It is immediately obvious, as judged by pronounced deviations from linearity for all of the curves depicted in Figure 3b, that **G**$_2$**NDS** is significantly more selective than **G**$_2$**BPDS** with respect to its inclusion of xylenes. The selectivity preference of **G**$_2$**NDS** for the xylene isomers decreases in the order *p*-xylene ≫ *o*-xylene > *m*-xylene. Initial stock solutions with large amounts of *m*-xylene (X_{m-xyl} > 0.7), however, tended to yield xylene-free material and so this concentration regime is not represented in the data for pairwise experiments with *m*-xylene. The absence of *m*-xylene inclusion most likely reflects the inability of this isomer to achieve favorable packing with the **G**$_2$**NDS** host. The apparent absence of *p*-xylene and *o*-xylene inclusion for X_{m-xyl} > 0.7 most likely reflects slow crystallization kinetics of the *p*-xylene and *o*-xylene inclusion compounds, relative to precipitation of the apohost or a short-lived methanol solvate, when these isomers are present at low concentrations under the crystallization conditions employed here. Pairwise competition between *p*-xylene and *m*-xylene reveals that *p*-xylene is included almost exclusively, with a selectivity coefficient of $K_{p-xyl:m-xyl}$ = 160, if the initial conditions are in the range 0.3 < X_{p-xyl} < 1. Such selectivity is considerably greater than that typically exhibited by industry-standard zeolitic materials for the separation of xylenes, for which the selectivity coefficients are less than 10.[1] Under the crystallization conditions employed here, the selectivity decreases dramatically for X_{p-xyl} < 0.3 and cannot be measured if X_{p-xyl} ≤ 0.1, reflecting the inability of **G**$_2$**NDS** to form inclusion compounds at high concentrations of *m*-xylene or low concentrations of *p*-xylene. Similar selectivity behavior is observed for the *p*-xylene/*o*-xylene competition, with a selectivity coefficient of $K_{p-xyl:o-xyl}$ = 36 for 0.3 < X_{p-xyl} < 1. At lower X_{p-xyl}, the selectivity for *p*-xylene falls steeply with decreasing X_{p-xyl}, becoming negligible at X_{p-xyl} = 0.1. Based on the crystal structures of **G**$_2$**NDS** inclusion compounds with the guests, it is reasonable to suggest that the pronounced change in selectivity is due to an architectural crossover of the bulk host structure (bilayer to brick) at X_{p-xyl} < 0.3. Notably, the *m*-xylene isomer was only included in the **G**$_2$**NDS** host when the other two isomers were present in significant quantities, indicating that *m*-xylene can only be entrained as an "impurity" in the inclusion compounds of either **G**$_2$**NDS**·(*p*-xylene) or **G**$_2$**NDS**·3(*o*-xylene). The selectivity of **G**$_2$**NDS** for *o*-xylene/*m*-xylene is modest, with a selectivity coefficient of $K_{o-xyl:m-xyl}$ = 5.4 in the concentration range where inclusion compounds can be obtained (0.3 < X_{o-xyl} < 1). Finally, crystallization from solutions containing an equimolar ratio of all three isomers produces an inclusion compound that is enriched almost

(18) Desiraju, G. R.; Gavezzotti, A. *Acta Crystallogr., Sect. B* **1989**, *B45*, 473−482.

(19) The unit cell volumes (V_{cell}) of **GS** structures correlate directly with the volume available for the inclusion of guests (V_{inc}). In the brick architecture, V_{inc} and V_{cell} depend on θ_{IR} according to a simple algebraic function, and the maximum unit cell volume can be determined from the first derivative $dV_{cell}/d\theta_{IR}$. For **G**$_2$**NDS**, the maximum achievable unit cell volume (normalized to Z = 2) is roughly 1990 Å^3, a value that would be achieved at a θ_{IR} value of 126°. See ref 14b.

Table 1. Summary of Crystallographic Data for Reported Compounds

compound	**G$_2$NDS**·(*p*-xylene)[16]	**G$_2$NDS**·3(*o*-xylene)[16]	**G$_2$BPDS**·(1,2-DMN)	**G$_2$BPDS**·(1,5-DMN)
formula	$C_{20}H_{28}N_6O_6S_2$	$C_{36}H_{48}N_6O_6S_2$	$C_{13}H_{16}O_3N_3S_1$	$C_{13}H_{16}O_3N_3S_1$
formula wt	512.60	724.92	294.35	294.35
crystal system	triclinic	monoclinic	triclinic	triclinic
space group	$P\hat{1}$	$P2_1/n$	$P\hat{1}$	$P\hat{1}$
color	colorless	colorless	colorless	colorless
a (Å)	7.2609(9)	7.5334(6)	7.221(1)	7.3080(4)
b (Å)	7.4075(9)	12.2651(9)	7.516(1)	7.4666(5)
c (Å)	13.154(2)	20.621(2)	14.923(2)	15.0563(9)
α (deg)	89.189(2)	90	88.007(2)	90.319(1)
β (deg)	77.186(2)	96.645(1)	82.683(2)	97.553(1)
γ (deg)	62.193(2)	90	61.762(2)	118.995(1)
V (Å^3)	560.98(2)	1892.5(3)	707.4(2)	710.08(7)
temp (K)	173(2)	173(2)	173(2)	173(2)
Z	1	2	2	2
R_1 [$I > 2\sigma(I)$]	0.0343	0.0403	0.0639	0.0681
wR_2 [$I > 2\sigma(I)$]	0.0941	0.1110	0.1894	0.1692
G.O.F.	1.075	1.022	1.099	1.001

compound	**G$_2$BPDS**·3(1,6-DMN)	**G$_2$BPDS**·$^3/_4$(1,7-DMN)[a]	**G$_2$BPDS**·(1,8-DMN)[a]	**G$_2$BPDS**·3(2,3-DMN)
formula	$C_{25}H_{28}N_3O_3S_1$	$C_{23}H_{29}N_6O_6S_2$	$C_{26}H_{32}N_6O_6S_2$	$C_{25}H_{28}N_3O_3S_1$
formula wt	450.56	549.64	588.70	450.56
crystal system	monoclinic	triclinic	orthorhombic	monoclinic
space group	$P2_1/n$	$P\hat{1}$	$Pna2_1$	$P2_1/n$
color	colorless	colorless	colorless	colorless
A (Å)	7.5289(4)	6.2313(8)	17.348(2)	7.5509(7)
B (Å)	12.4257(7)	7.177(1)	7.4584(5)	25.493(2)
C (Å)	25.421(2)	14.736(2)	21.626(2)	12.057(2)
α (deg)	90	78.793(2)	90	90
β (deg)	95.539(1)	89.763(2)	90	91.574(2)
γ (deg)	90	86.279(2)	90	90
V (Å^3)	2367.0(2)	645.1(2)	2798.2(3)	2320.1(4)
temp (K)	173(2)	173(2)	173(2)	173(2)
Z	4	1	4	4
R_1 [$I > 2\sigma(I)$]	0.0759	0.0584/0.0410	0.0703/0.0452	0.0430
wR_2 [$I > 2\sigma(I)$]	0.2292	0.1762/0.1121	0.2227/0.0627	0.0889
G. O. F.	1.06	1.068	0.982	0.842

compound	**G$_2$BPDS**·3(2,6-DMN)	**G$_2$BPDS**·(2,6-DMN)	**G$_2$BPDS**·3(2,7-DMN)
formula	$C_{25}H_{28}N_3O_3S_1$	$C_{26}H_{32}N_6O_6S_2$	$C_{75}H_{84}N_9O_9S_3$
formula wt	450.56	588.70	1351.69
crystal system	monoclinic	monoclinic	monoclinic
space group	$P2_1/n$	$C2/c$	Cm
color	colorless	colorless	Colorless
A (Å)	7.5382(5)	31.569(2)	13.8540(9)
B (Å)	25.544(2)	7.3560(5)	77.733(5)
C (Å)	11.9693(8)	12.7025(9)	7.5814(5)
α (deg)	90	90	90
β (deg)	92.656(1)	109.611(3)	121.055(1)
γ (deg)	90	90	90
V (Å^3)	2302.3(3)	2778.7(3)	6994.3(8)
temp (K)	173(2)	173(2)	173(2)
Z	4	4	4
R_1 [$I > 2\sigma(I)$]	0.0384	0.0453	0.0473
wR_2 [$I > 2\sigma(I)$]	0.0979	0.1161	0.1087
G.O.F.	1.046	1.005	0.994

[a] The two agreement (R) factors given correspond to two separate refinements of the X-ray data, the latter being based upon a "framework only" refinement facilitated with the SQUEEZE subroutine of PLATON.[32] This type of refinement confirms that the poor residuals from the traditional refinement are associated primarily with poor modeling of the disordered guests and allows calculation of the electron density associated with these guests.

exclusively in *p*-xylene ($Y_{p-xyl} > 0.95$). This represents almost complete separation of *p*-xylene from the other isomers in a single crystallization step!

The different xylene inclusion selectivity profiles for **G$_2$BPDS** and **G$_2$NDS** in Figure 3 demonstrate the ability to tailor separations by simply changing the organodisulfonate pillar of the **GS** host. It is important to recognize that while **G$_2$BPDS** proved to be ineffective at separating the xylene isomers, it was not necessary to design an entirely new host system to achieve effective separations. Rather, a more appropriate host was simply selected from a homologous library. The observation of poor selectivity for the isostructural **G$_2$BPDS** xylene inclusion compounds, but substantial selectivity for the xylene inclusion compounds of **G$_2$NDS**, suggests that inclusion selectivity will be most pronounced when the host architectures differ. This is perhaps not surprising as different crystallization kinetics and thermodynamics would be expected for the different architectures. It is apparent that the ability of the **GS** hosts to adopt multiple architectures is a highly desirable feature with respect to the achievement of selective inclusion, with host−guest combinations that straddle the steric threshold between bilayer and

brick architectures providing the best opportunities for inclusion-based separations.

Selective Inclusion of Dimethylnaphthalenes. Mixtures of dimethylnaphthalenes (DMNs) are produced in substantial quantities during coal liquefaction, but their refinement by conventional means—distillation, solvent extraction, and fractional crystallization—is difficult owing to the similar physical properties of the individual isomers. The difficulties of separation are reflected in the retail cost of the individual pure isomers relative to the cost of a mixture (e.g., $158/g for 1,7-DMN, $118/g for 2,7-DMN, $29/g for 2,6-DMN, as compared to $0.10/g for a mixture of isomers; Aldrich, year 2000). The 2,6-DMN isomer is of particular interest because it can be readily converted to 2,6-naphthalenedicarboxylic acid and subsequently polyethylene naphthalate, a valuable thermotropic liquid crystal polymer used for the manufacture of specialty synthetic fibers and functional resins with desirable thermal and mechanical properties.[20] Synthetic efforts aimed at producing pure DMNs can be plagued by the poor regioselectivity of alkylation. Various methods for the bulk separation of DMN isomers have been attempted. The use of porous zeolites has met with limited success.[21] Various means of cocrystallization have been employed, including the selective inclusion of 2,3-DMN in a thiourea and the specific cocrystallization of 2,6-DMN with flumethrin.[22,23] Liquid−liquid extractions that rely on the formation of supramolecular complexes of 2,6-DMN with a modified α-cyclodextrin have been reported to be somewhat effective for separating 2,6-DMN/2,7-DMN.[24] Carbon nanotubes have also been proposed as a selective absorbent medium for DMNs, the nanotubes discriminating for the isomers on the basis of their different molecular diameters.[25] Though each of these examples has its limitations, they suggest the feasibility of separating DMN isomers through carefully designed molecular recognition, coupled with crystallization.

A complete analysis of the inclusion selectivity of a particular **GS** host toward the DMN isomers would require the determination of all 45 possible pairwise selectivity profiles. Therefore, an initial, less laborious, assay was performed wherein the isomeric distribution of a commercial mixture of DMNs was compared with that of inclusion compounds retrieved from a methanol solution containing a **GS** host and the commercial DMN mixture. Four hosts of varying pillar lengths, namely **G_2NDS**, **G_2BPDS**, **G_2ADS**, and **G_2ABDS**, were assayed (Figure 5). With the exception of the peak at ca. 54.2 min, which is a composite of the contributions from the 2,3-, 1,4-, and 1,5-DMN isomers, all ten DMN isomers can be resolved by gas chromatography on a Supelco Beta-Dex capillary column. Analyses using an All Tech column allowed determination of the individual amounts of 2,3-, 1,4-, and 1,5-DMN, as exemplified in Figure 6. That both columns, each endowed with more than 100 000 theoretical plates, were necessary for the resolution and identification of all 10 isomers further illustrates the difficulties in separating DMNs. Quantitative isomer distributions, including the relative amounts of each of the 10 isomers obtained by integration of the chromatograph peaks, are plotted as histograms in Figure 7.

It is clear from Figures 5−7 that, of the four hosts subjected to the assay, **G_2BPDS** displays the greatest selectivity with respect to its inclusion of DMN isomers. Indeed, under the conditions of the experiment, **G_2BPDS** includes only four of the 10 isomers, namely, 2,6-, 2,7-, 1,6-, and 2,3-DMN, whereas the other hosts include significant amounts of almost every isomer. Moreover, Figure 7 illustrates that the mole fractions of 2,6-, 2,7-, and 2,3-DMN included within **G_2BPDS** are greater than their corresponding initial solution values, but the mole fraction of 1,6-DMN is diminished significantly. This clearly indicates that, of the four included isomers, 1,6-DMN is the least preferred. Notably, the chromatographic trace derived from the inclusion compound of **G_2ADS** strongly resembles that obtained using **G_2BPDS**. The similarity is perhaps not surprising given that **BPDS** and **ADS** have similar lengths (10.6 and 10.8 Å, respectively, as measured by the intramolecular sulfur−sulfur distances) and similar inclusion cavity volumes.[14b] The two hosts differ significantly, however, with respect to the inclusion of 1,4-, 1,5-, and 2,3-DMN; whereas **G_2BPDS** exclusively includes 2,3-DMN among this group, **G_2ADS** includes all three isomers (Figure 6b). **G_2NDS** and **G_2ABDS** are much less selective than either **G_2BPDS** or **G_2ADS**. It is perhaps not surprising that **G_2ABDS** exhibits poor selectivity, since, given the length of the pillar, it is likely that this host forms inclusion compounds with DMN isomers that are all of the bilayer structure type. **G_2NDS** appears to be somewhat selective, however, toward the inclusion of certain 1,*n*-DMN isomers versus 2,*n*-DMNs.

To elucidate the structural origins associated with the apparent inclusion selectivity, single-crystal structures were determined, where possible, for the **G_2BPDS**·*n*(DMN) series of inclusion compounds (Figure 8). This series was chosen for structural studies because, of the four hosts assayed, **G_2BPDS** exhibited the greatest selectivity for inclusion of DMNs and was therefore most likely to reveal any possible relationship between selectivity and structure. With the exception of 1,3-DMN and 1,4-DMN, **G_2BPDS** forms inclusion compounds with any of the DMN isomers when crystallized from methanolic solutions containing the appropriate guest. All attempts at forming **G_2BPDS** inclusion compounds of 1,3-DMN and 1,4-DMN yielded only the methanol clathrate.[14d]

(20) (a) Barber, J. B.; Siddiqui, A. A. *Polym. Prepr.* **1998,** *39*, 648. (b) Ohno, M.; Toshikazu, T.; Endo, T. *J. Polym. Sci., Part A* **1995,** *33*, 2647.

(21) (a) Inui, T.; Pu, B. *Sep. Technol.* **1995,** *5*, 229. (b) Ellis, L.; Alexander, R.; Kagi, R. I. *Org. Geochem.* **1994**, *21*, 849. (c) Maki, T.; Yokoyama, T.; Nakanishi, A. Japanese Patent 63-135341, 1988. (d) Maki, T.; Yokoyama, T.; Nakanishi, A. Japanese Patent 63-146834, 1988. (e) Maki, T.; Yokoyama, T.; Nakanishi, A. Japanese Patent 63-150233, 1988. (f) Maki, T.; Yokoyama, T.; Nakanishi, A. Japanese Patent 1-168627, 1988. (g) Iwai, Y.; Uchida, H. Mori, Y.; Higashi, H.; Matsuki, T.; Furuya, T.; Arai, Y.; Yamamoto, K.; Mito, Yutaka, M. *Ind. Eng. Chem. Res.* **1994**, *33*, 2157.

(22) (a) Miyashi, T.; Yamashita, Y.; Suzuki, T.; Fujii, H. European Application EP 346843, 1989. (b) Hiroshi, O.; Oshima, Y.; Shindo, T.; Katsuhiko, S.; Katahira, S.; Koishi, H. Japanese Patent JP 02240030, 1990.

(23) Born, L.; Fuchs, R. *Angew. Chem., Int. Ed. Engl.* **1991**, *30*, 1634.

(24) (a) Uemasu, I. *Value Adding Solvent Extr.* **1996**, *2* 1635−1640. (b) Uemasu, I. *Jpn. Kokai Tokkyo Koho* **1994**, 4.

(25) Takaba, H.; Katagiri, M.; Kubo, M.; Vetrivel, R.; Miyamoto, A. *Micropor. Mater.* **1995**, *3*, 449−455.

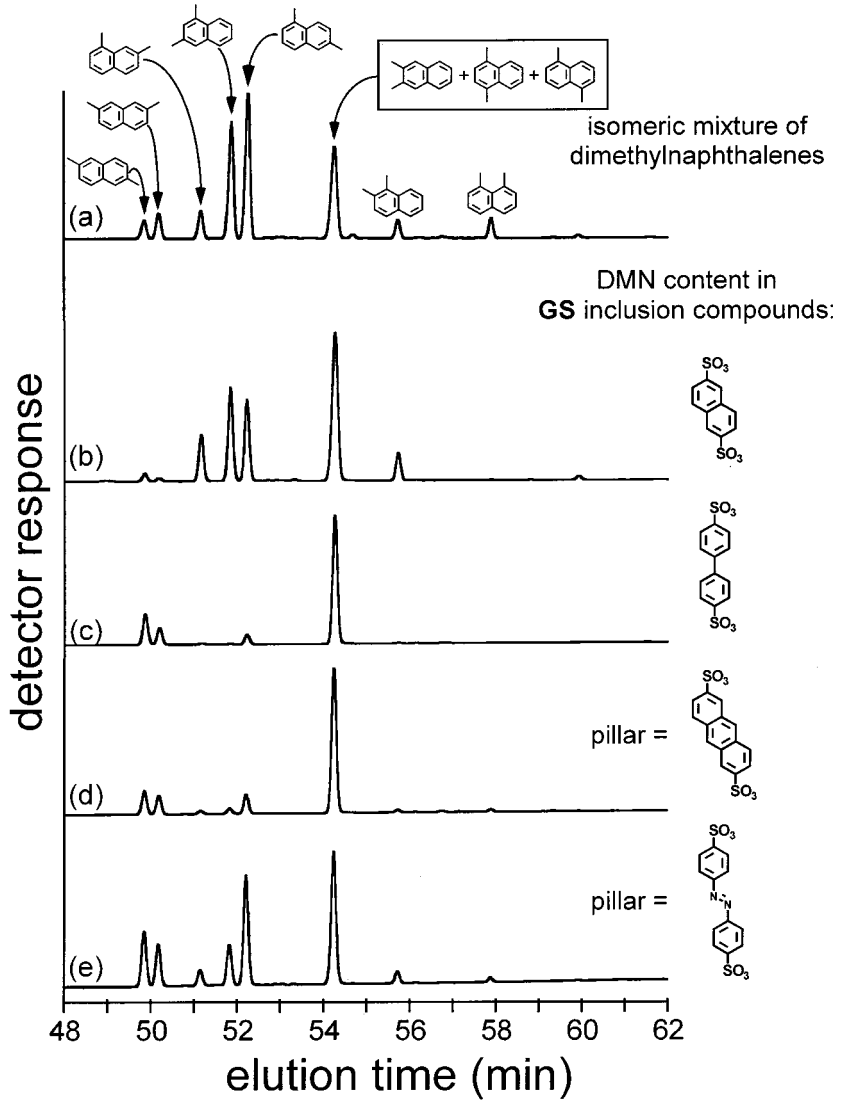

Figure 5. Gas chromatograms, as analyzed using a Supelco Beta-Dex capillary column, indicating the DMN isomer distribution in (a) a commercial mixture (Aldrich) that was used for selectivity studies, and (b−e) the corresponding inclusion compounds as retrieved from individual methanolic solutions containing the commercial mixture and **G_2BPDS**, **G_2NDS**, **G_2ADS**, and **G_2ABDS** apohosts.

The most striking observation is the essentially isostructural character of the **G_2BPDS** inclusion compounds of 1,6-, 2,3-, 2,6-, and 2,7-DMN, the four guests included selectively by the host in the aforementioned preliminary assay (Figure 8a-d). The single crystal structure of each compound is nearly orthorhombic, each exhibiting a 1:3 host:guest stoichiometry with the host adopting the simple brick architecture and slightly puckered **GS** sheets ($\theta_{IR} = 136-142°$). Like **G_2NDS**·3(*o*-xylene), the **BPDS** pillars and DMN guests in these inclusion compounds also adopt a herringbone packing arrangement between the **GS** sheets. Although the structures of **G_2BPDS**·3(2,6-DMN) and **G_2BPDS**·3(2,3-DMN) are essentially identical, the structure of **G_2BPDS**·3(1,6-DMN) is slightly different in that the unique angle (β) occurs between the "ribbon" direction and a vector nearly orthogonal to the **GS** sheet, rather than the direction corresponding to a_1 and b_1 within the plane of the **GS** sheet as depicted in Scheme 2. The most obvious difference between these structures and that of **G_2BPDS**·3(2,7-DMN) is a tripling of the unit cell axis that corresponds to the direction normal to the **GS** sheets; subtle differences in pillar guest packing in alternating layers reduce the overall symmetry of the crystal.

G_2BPDS·(1,8-DMN) also adopts the brick host architecture, but the **GS** sheets are more highly puckered ($\theta_{IR} = 93°$), thereby reducing the inclusion cavity volume and resulting in a compound of 1:1 host:guest stoichiometry. The remaining **G_2BPDS** inclusion compounds of 1,2-, 1,5-, and 1,7-DMN adopt structures wherein the host exhibits the discrete bilayer architecture. Of these compounds **G_2BPDS**·(1,5-DMN) and **G_2BPDS**·(1,2-DMN) are isostructural, possessing one-dimensional channels that are filled with disordered DMN guests. **G_2BPDS**·$^3/_4$(1,7-DMN) (not shown) differs from **G_2BPDS**·(1,5-DMN) and **G_2BPDS**·(1,2-DMN) with respect to the **GS** sheets, exhibiting the "shifted-ribbon" hydrogen bonding motif rather than the "quasihexagonal" pattern illustrated in Scheme 2. The host structure therefore closely resembles that of the aforementioned **G_2BPDS**·(xylene) inclusion compounds, but with a 1:0.75 host:

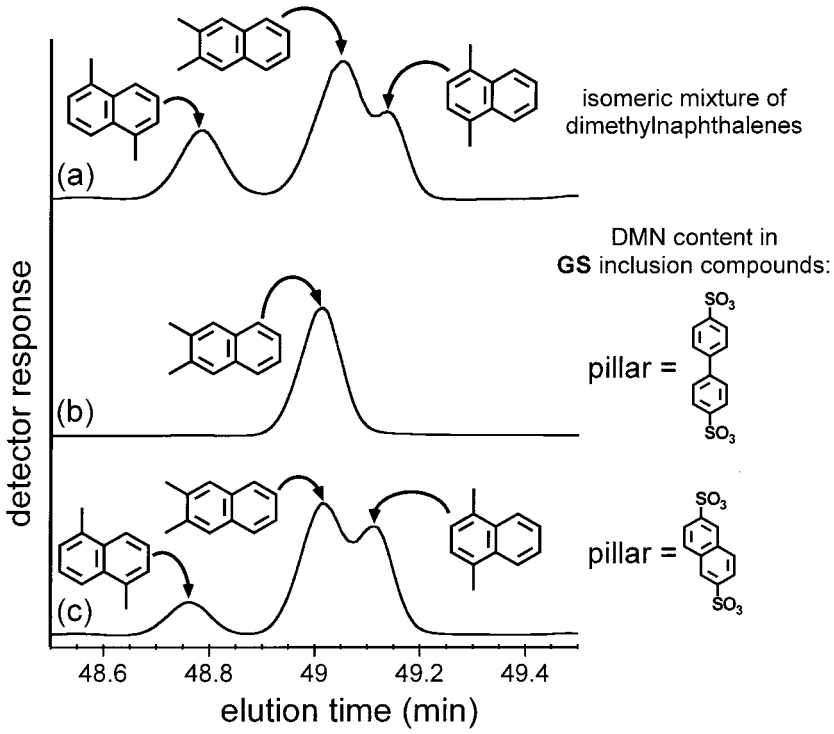

Figure 6. (a) A gas chromatogram, using an All Tech EC−Wax capillary column, of a commercial mixture of all 10 DMN isomers, illustrating here only the amounts of the 1,5-, 2,3-, and 2,4- isomers. (b,c) Gas chromatograms indicating the DMN isomers included and retrieved from individual crystallization solutions containing the **G_2BPDS** and **G_2NDS** apohosts.

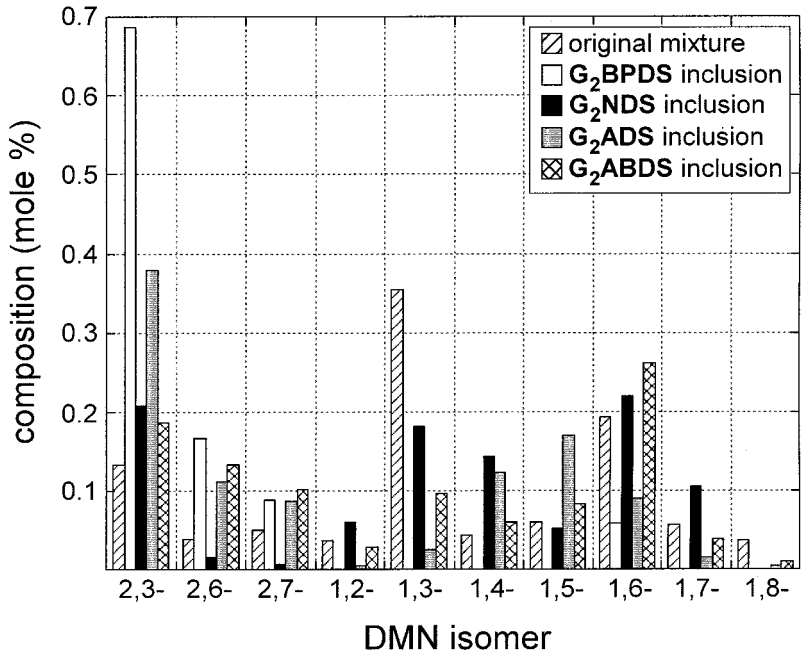

Figure 7. Histogram of DMN isomer distributions in an original commercial mixture and in the inclusion compounds of four **GS** hosts grown from a methanolic solution containing the same mixture.

guest stoichiometry[26] and completely disordered 1,7-DMN guest molecules occupying the channels of the host.

Interestingly, 2,6-DMN occasionally formed **G_2BPDS**·(2,6-DMN), a 1:1 inclusion compound wherein the host adopts the bilayer architecture (Figure 9). It was difficult, however, to crystallize this phase reproducibly. Though we have characterized over 200 **GS** inclusion compounds with various combinations of organodisulfonate pillars and guests, **G_2BPDS**·(2,6-DMN) and **G_2BPDS**·3(2,6-DMN) are the only **GS** architectural isomers occupied by the same guest molecule. Unlike a great majority of other **G_2BPDS** inclusion compounds, the biphenyl pillars in **G_2BPDS**·(2,6-DMN) are significantly "bowed", with S···centroid···S angles measuring 167.5°. This structural distortion, which does not lead

(26) The 1:$^3/_4$ host:guest stoichiometry was established by ^{1}H NMR spectroscopy, thermal gravimetric analysis, and analysis of the residual electron density, using SQUEEZE, within the channels of the fully refined **G_2BPDS** host framework.

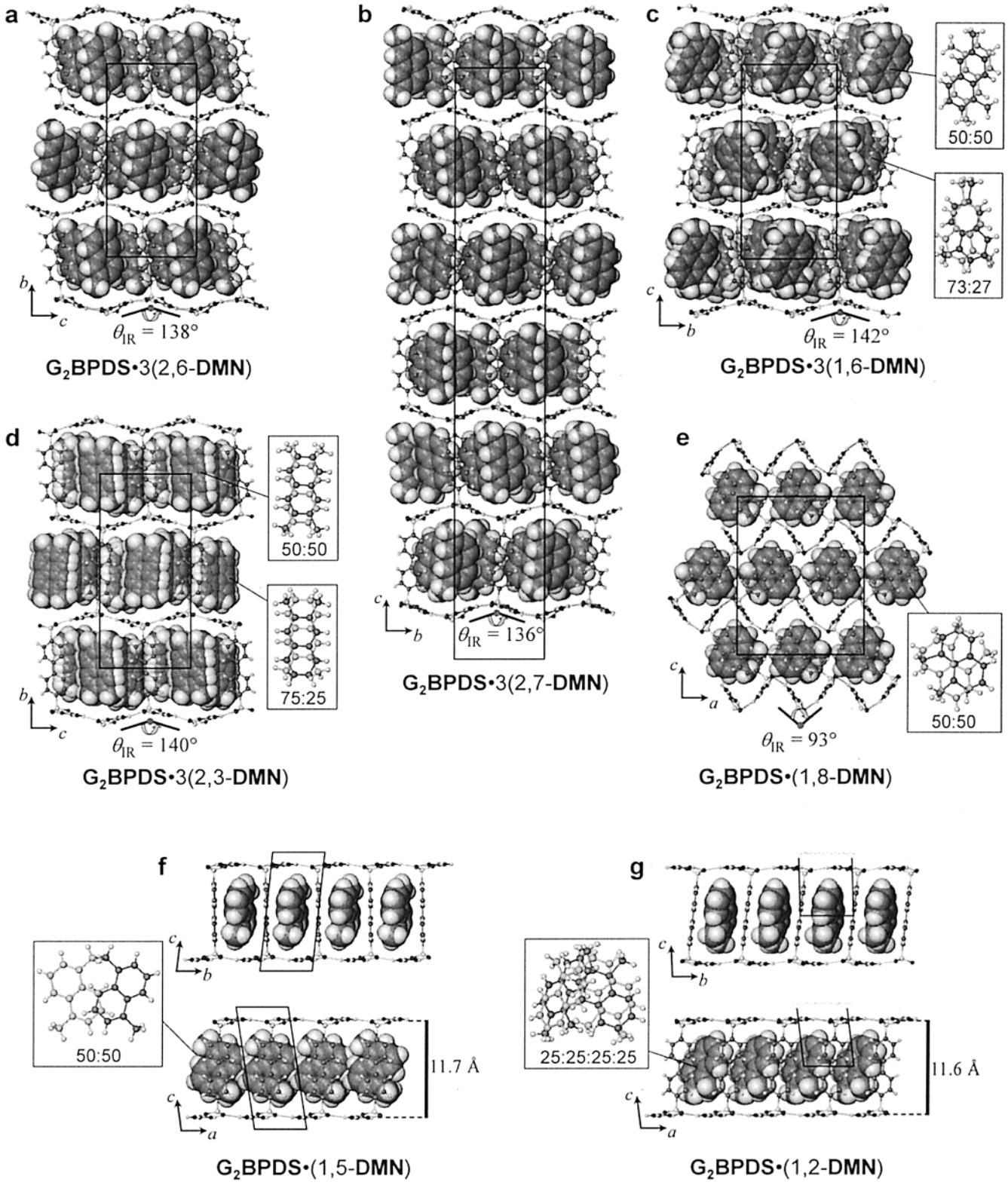

Figure 8. Single-crystal structures, as viewed parallel to the **GS** sheets, of (a) simple brick **G**$_2$**BPDS**·3(2,6-DMN) (θ_{IR} = 138°), (b) simple brick **G**$_2$**BPDS**·3(2,7-DMN) (θ_{IR} = 136°), (c) simple brick **G**$_2$**BPDS**·3(1,6-DMN) (θ_{IR} = 142°), (d) simple brick **G**$_2$**BPDS**·3(2,3-DMN) (θ_{IR} = 140°), (e) highly puckered simple brick **G**$_2$**BPDS**·(1,8-DMN) (θ_{IR} = 93°), (f) bilayer **G**$_2$**BPDS**·(1,5-DMN), and (g) bilayer **G**$_2$**BPDS**·(1,2-DMN). The dimethylnaphthalene guests in many of these inclusion compounds are disordered. In all such compounds depicted here, the disorder of the guest could be resolved to the extent that the different guest orientations could be definitively established. These orientations and the corresponding occupancies (%) are depicted in the rectangular boxes. The dimethylnaphthalene guests of the bilayer inclusion compound **G**$_2$**BPDS**·(1,7-DMN) (not shown) are extremely disordered and could not be resolved.

to an appreciable increase in the bilayer height or the normalized unit cell volume relative to the other bilayer compounds, is apparently required in order to optimize packing between the 2,6-DMN guests and the **BPDS**

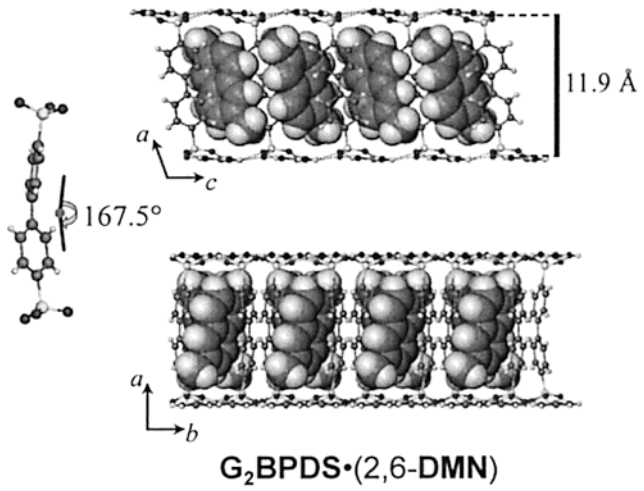

Figure 9. The crystal structure of the bilayer inclusion compound **BPDS**·(2,6-DMN) as viewed along the [010] (top) and [001] (bottom) directions. The **BPDS** pillars are significantly distorted from linearity (left).

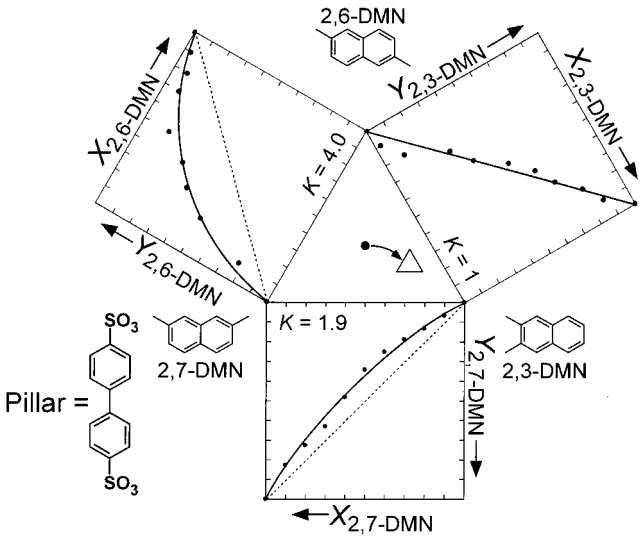

Figure 10. Selectivity profiles for the inclusion of 2,3-, 2,6-, and 2,7-DMN isomers by **G**$_2$**BPDS**. The offset of the triangle from the filled circle in the center denotes the selectivity observed when competition experiments are performed with an equimolar mixture of all three isomers.

pillars while maintaining the geometric constraints imposed by the **GS** sheets. Bowing of the **BPDS** pillar to the degree observed here should not be regarded as energetically prohibitive, as there is significant precedent for much more strained aromatic rings systems, for example the bowing of biphenyl moieties on the surface of C_{60} is 122° (measured using the same convention).[27] Nevertheless, this structural distortion may be partially responsible for the infrequent and uncontrollable formation of the bilayer **G**$_2$**BPDS**·(2,6-DMN) structure, which we suspect is a kinetically preferred phase under some as-of-yet unidentified conditions.

The observation that the inclusion compounds of the four preferentially included DMN isomers adopt similar brick structures (Figure 8a−d) might be construed to signify that the slightly puckered simple brick host architecture is more thermodynamically favored than the highly puckered brick of **G**$_2$**BPDS**·(1,8-DMN) or the bilayer architectures adopted by the remaining **G**$_2$**BPDS** inclusion compounds of DMN. It is likely that this reflects the difficulty of 1,*n*-DMN isomers to pack efficiently in the herringbone motif within the confines of the **GS** brick architecture, owing to a steric hindrance imposed by the 1-methyl groups. This is further supported by the fact that that 1,6-DMN is the least preferred of the four included DMN isomers. It must be noted, however, that while the preliminary assay depicted in Figure 5 is practical, it should be used only as a guide for deducing the efficacy of a particular host toward the selective inclusion of DMN isomers. It is possible that inclusion selectivity, as deduced from the assay rather than by pairwise competitions, is influenced by kinetic factors such as nucleation and growth rates that can be affected by the individual concentrations of guests in the crystallization medium. The original commercial mixture, for example, contains significantly greater quantities of 1,6-, 1,3-, and 2,3-DMN relative to the other isomers. The 1,3-DMN isomer does not form inclusion compounds with **G**$_2$**BPDS**, but it is conceivable that the relatively high concentrations of 1,6- and 2,3-DMN in the commercial mixture facilitates the nucleation of the slightly puckered brick host architecture, subsequently leading to facile inclusion of 2,6-DMN, 2,7-DMN, 1,6-DMN, and 2,3-DMN relative to the other isomers.

Among the four DMN isomers included by **G**$_2$**BPDS**, 1,6-DMN is clearly the least preferred. Pairwise competition experiments were thus performed in order to evaluate the relative inclusion preference of **G**$_2$**BPDS** among 2,6-, 2,7-, and 2,3-DMN (Figure 10). It is not surprising that, given the essentially identical structures of their corresponding inclusion compounds, **G**$_2$**BPDS** is unable to discriminate between 2,3- and 2,6-DMN. The 2,3-DMN/2,7-DMN selectivity is modest, but improved, with an average selectivity coefficient of $K_{2,3:2,7} = 1.9$ The selectivity in the 2,6-DMN/2,7-DMN competition experiments is even greater, with **G**$_2$**BPDS** exhibiting a preference for 2,6-DMN with $K_{2,6:2,7} = 4.0$. The improved selectivity for 2,3-DMN and 2,6-DMN may stem from the somewhat different structures of their inclusion compounds, compared to **G**$_2$**BPDS**·3(2,7-DMN) which has a unit cell roughly three times larger that that of the other two inclusion compounds. It is conceivable that this may be manifested in a larger critical nucleus size, and a corresponding lower nucleation rate, for **G**$_2$**BPDS**·3(2,7-DMN).

It should be noted that 2,6- and 2,7-DMN are the most difficult to separate among the DMN isomers using conventional methods.[28] The observed inclusion selectivity for these two isomers, using the solution/inclusion equilibrium data in a manner analogous to a McCabe−Thiele liquid/vapor diagram,[29] suggests that 2,6-DMN in greater than 94% purity can be achieved in three successive crystallization steps from an initial mixture containing only 20% 2,6-DMN (Figure 11).

(27) Hirsch, A. *The Chemistry of Fullerenes*; G. Theime Verlag: Stuttgart, 1994.

(28) (a) Kabot, F. J.; Ettre, L. S. *Anal. Chem.* **1964**, *36*, 250. (b) Min, X.; Bruner, F. *J. Chromatogr.* **1989**, *468*, 365. (c) Andrews, A. R. J.; Wu, Z.; Zlatkis, A. *Chromatographia* **1992**, *34*, 163.

(29) Thiele, E. W.; Geddes, R. L. *Ind. Eng. Chem.* **1933**, *25*, 289.

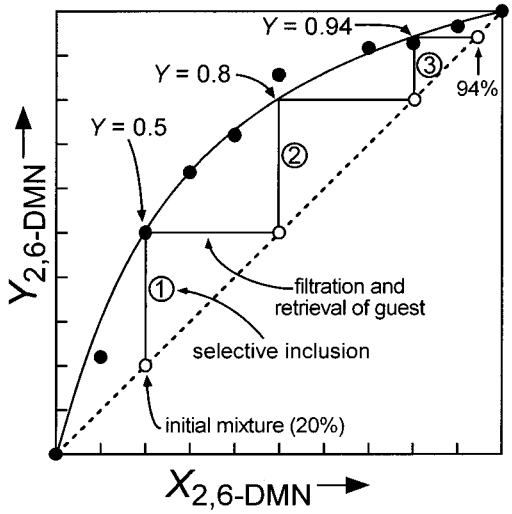

Figure 11. A McCabe−Thiele type plot illustrating that a sample of 2,6-DMN (94% pure) can be obtained in only three crystallization/filtration steps from an initial mixture containing only 20% 2,6-DMN and 80% 2,7-DMN.

Conclusions

The selective inclusion behavior described here illustrates the potential for crystallization-based separations based on inclusion phenomena. The lamellar **GS** hosts are exemplary in this respect because, unlike most other hosts, they can be modified in a systematic manner with retention of the general structural features, and thus comprise a library of homologous hosts that can be explored to attain an optimum separation protocol. The **GS** hosts can also accommodate a broad range of differently sized and shaped guests owing to their inherent conformational flexibilty and architectural isomerism. The data obtained here suggest that separations that are otherwise difficult with conventional approaches can be achieved effectively with this strategy. Furthermore, the low density of the host frameworks enables a substantial amount of guest inclusion, up to 52% by mass for the compounds reported here.

Experimental Section

Materials. Solvents, xylenes, dimethylnaphthalenes, and disodium 2,6-naphthalenedisulfonate were used as received from Aldrich (Milwaukee, WI). 4,4-Biphenyldisulfonic acid was purchased from TCI America. The potassium salt of 2,6-anthracene disulfonate[30] and 4,4′-azobenzenedisulfonic acid[14f] were prepared according to published procedures. Metal salts of the sulfonic acids were converted to the acid form by passing them through an Amberlyst 36(wet) ion-exchange column. **G_2NDS**, **G_2BPDS**, **G_2ADS**, and **G_2ABDS** precipitate, as acetone clathrates, by direct reaction of guanidinium tetrafluoroborate, prepared by neutralization of guanidinium carbonate with tetrafluoroboric acid, with the corresponding disulfonic acid in acetone. These compounds readily lose enclathrated acetone under ambient conditions to yield pure guanidinium organodisulfonate apohosts. Single crystals for X-ray diffraction were obtained from methanolic solutions containing the dissolved **GS** apohost and the corresponding guest where applicable. In addition to single-crystal X-ray diffraction, the stoichiometry of guest inclusion was determined by ^{1}H NMR (Varian INOVA 200 MHz spectrometer) or thermal gravimetric analysis (Perkin-Elmer TGA 7).

X-ray Crystallography. Single-crystal structures of inclusion compounds were determined at −100 °C using either a Siemens or Bruker CCD platform diffractometer with graphite monochromated Mo−Kα radiation (λ_= 0.71073 Å). The structures were solved by direct methods and refined with full-matrix least-squares/difference Fourier analysis using the SHELX-97−2 suite of software.[31] Where appropriate, all non-hydrogen atoms were refined with anisotropic displacement parameters and all hydrogen atoms were placed in calculated positions and refined with a riding model. Data were corrected for the effects of absorption using SADABS. Due to considerable disorder of the guest molecules, the data collected from samples of **G_2BPDS**·(1,8-DMN) and **G_2BPDS**·(1,7-DMN) were each subjected to two refinements, one of which is refined with the exclusion of the guest using the SQUEEZE subroutine of PLATON.[32] Experimental details of the crystal structure determinations are compiled in Table 1. Single crystals of the inclusion compounds suitable for X-ray structure determination were prepared under ambient conditions by slow evaporation of methanolic solutions containing the appropriate host and guest components.

Inclusion Selectivity. A prepared iomeric mixture (with mole fractions ranging from 0.0 to 1.0) of two potential guests was added, in an approximate 20-fold excess, to a methanolic solution of the guanidinium organodisulfonate host. Crystallization of the corresponding inclusion compounds commenced upon standing or after slow evaporation of some solvent. After approximately 25% of the total host material had precipitated from solution, the resulting crystals were harvested by filtration and washed briefly with cold methanol (to remove surface residue). The crystals were then dissolved in methanol, and the solution was evaluated for isomer composition by gas chromatographic (GC) analysis. Whenever the quality of the crystalline inclusion compounds permitted, the data obtained from batches of crystalline material were compared to data that could be obatined from what were seemingly individual single crystals. In all cases the results were essentially identical. For selected experiments, inclusion compounds were crystallized in the presence of equimolar concentrations of three guests, or, as with the DMN separations, a commercially available mixture (Aldrich) of all isomers. The resulting mole fractions obtained from the GC results were reproducible, within 4%, among different crystallization experiments.

Gas Chromatography. Gas chromatographic analyses were performed with an HP 6890 series instrument using helium carrier gas and a flame ionization detector. The inlet and detector were held at constant temperatures of 200 °C and 250 °C, respectively, for all analyses. Complete resolution of xylene isomers was achieved with an All Tech Econocap capillary column (30m × 25 mm diameter × 0.25 μm stationary phase of EC−Wax) using a constant 1 mL/min flow rate and 150 °C. This afforded elution times of: 4.451, 4.576, and 5.560 min for the *p*-xylene, *o*-xylene, and *m*-xylene, respectively. Determination of the relative amounts of the dimethylnaphthalenes (DMNs) required a protocol that relied on both the All Tech Econocap column and a Supelco U Beta-Dex 120 column (60m × 0.25 mm diameter x 25 μm stationary phase of 20% β-cyclodextrin embedded in a medium polarity film). The All Tech column was able to separate all but the 2,6- and 2,7-DMN isomers, and the Supelco column was able to separate all but the 1,4-, 1,5-, and 2,3-DMN isomers. The use of both columns in separate analyses, however, enabled determination of the relative amounts of all 10 DMN isomers. Analyses on the All Tech column were performed at a constant flow rate of 2.4 mL/min at 100 °C for 40 min, after which the temperature was increased by 5 °C/min up to 200 °C. The total analysis time was approximately 65 min. Analyses on the Supelco column were performed with a flow rate of 0.6 mL/

(30) Acquavella, M. F.; Evans, M. E.; Farraher, S. W.; Névoret, C. J.; Abelt, C. J. *J. Org. Chem.* **1994**, *59*, 2894−2897.

(31) *SHELX*-97, Sheldrick, G. M., University of Göttingen, 1997.

(32) Spek, A. L. *Acta Crystallogr.* **1990**, *A46*, C-34.

min at 140 °C for 40 min, after which the temperature was increased by 2 °C/min until all the isomers eluted. The total analysis time was approximately 62 min.

Acknowledgment. The authors gratefully acknowledge the financial assistance of the National Science Foundation (DMR-9908343) and the University of Minnesota National Science Foundation Materials Research Science and Engineering Center (DMR-9809364) and Dr. David Hacker (Argonne National Laboratory) for helpful discussions. K.T.H. wishes to thank NSERC Canada for a postdoctoral fellowship.

CM0104452